



HAL
open science

Temperature and pressure dependence of the Yb valence state in $\text{YbMn}_{\sim 0.17}\text{Si}_{\sim 1.89}$

Bodry Tegomo Chiogo, Nicolas P. Martin, Léopold V.B. Diop, Bernard Malaman, Daniel Malterre, François Baudelet, Lucie Nataf, Thomas Mazet

► To cite this version:

Bodry Tegomo Chiogo, Nicolas P. Martin, Léopold V.B. Diop, Bernard Malaman, Daniel Malterre, et al.. Temperature and pressure dependence of the Yb valence state in $\text{YbMn}_{\sim 0.17}\text{Si}_{\sim 1.89}$. *Journal of Applied Physics*, 2022, 132 (20), pp.205902. 10.1063/5.0125875 . hal-03891295

HAL Id: hal-03891295

<https://hal.science/hal-03891295>

Submitted on 9 Dec 2022

HAL is a multi-disciplinary open access archive for the deposit and dissemination of scientific research documents, whether they are published or not. The documents may come from teaching and research institutions in France or abroad, or from public or private research centers.

L'archive ouverte pluridisciplinaire **HAL**, est destinée au dépôt et à la diffusion de documents scientifiques de niveau recherche, publiés ou non, émanant des établissements d'enseignement et de recherche français ou étrangers, des laboratoires publics ou privés.

Temperature and pressure dependence of the Yb valence state in $\text{YbMn}_{-0.17}\text{Si}_{-1.89}$

B. Tegomo Chiogo,¹ N.P. Martin,¹ L.V.B. Diop,¹ B. Malaman,¹ D. Malterre,¹
F. Baudelet,^{2,†} L. Nataf,² and T. Mazet^{1,a}

¹*Université de Lorraine, CNRS, IJL, F-54000 Nancy, France*

²*Synchrotron SOLEIL, URI CNRS, Saint-Aubin BP 48, 91192 Gif-sur-Yvette, France*

Single crystals of the non-stoichiometric $\text{YbMn}_{-0.17}\text{Si}_{-1.89}$ intermetallic compound were investigated by room-temperature x-ray diffraction as well as by temperature and pressure dependent x-ray absorption experiments at the Yb L_3 edge. The crystal structure can be described in the orthorhombic space group $Cmcm$ or in the non-centrosymmetric $P2_1$ monoclinic space group. In both cases, the cell comprises two Yb sites of identical multiplicity with close coordination numbers and interatomic distances. The average Yb valence is found independent of temperature $v_{\text{av}} \sim 2.42$. Such a low Yb valence is hardly compatible with the occurrence of local magnetism on Yb inferred from a previous study. The pressure dependence of the Yb valence at 10 K does not reveal any first-order transition. The average Yb valence increases continuously under pressure but remains far from trivalency ($v_{\text{av}} \sim 2.63$) even under the highest external pressure used of 37 GPa.

I. INTRODUCTION

In intermetallics, ytterbium, as a few other rare-earth elements with unstable 4f shell like cerium or europium, may present a wealth of physical behaviors such as homogeneous intermediate valency, heavy-fermions, non-Fermi-liquid and quantum criticality.¹ They result from the close proximity of two electronic configurations ($4f^{13}$ and $4f^{14}$ for Yb) and the hybridization between the localized 4f states and the conduction electrons. In most cases, Yb is alloyed with non-magnetic elements. As proposed by Doniach,² the physics of such systems can be understood as arising from the competition between the Ruderman-Kittel-Kasuya-Yosida (RKKY) exchange interaction and the Kondo screening of the 4f moments with characteristic temperature T_{RKKY} and T_{K} , respectively. Both interactions depend on the 4f-conduction electron hybridization but in a different manner such that the ground state can be altered thanks to a control parameter like chemical composition, external pressure or magnetic field. In the case of Yb, high pressure favors the trivalent ($4f^{13}$) weakly hybridized state of lower atomic volume. The Yb sublattice may then magnetically orders but with an ordering temperature that rarely exceeds 5 K.^{1,3,4} The Yb magnetic moment is often reduced compare to the free ion value due to Kondo screening.^{1,3} For lower pressure (i.e. stronger

[†] 1963-2022

^a Author to whom correspondence should be addressed. Electronic mail: thomas.mazet@univ-lorraine.fr.

hybridization), the Kondo temperature T_K dominates the RKKY temperature, Yb is then in a non-magnetic intermediate valent state ($2 < v < 3$).

At absolute zero temperature, the point delineating the two ground states is a Quantum Critical Point (QCP).¹ It generally occurs for weakly hybridized nearly trivalent Yb ($v \sim 3$). Some 4f quantum critical materials deviate from this behavior, with the QCP sometimes completely detached to the 4f magnetic instability, and are said to be unconventional.^{5,6} They have been analyzed using, for instance, Kondo breakdown⁷ or critical valence fluctuations theories⁸. In the vicinity of a QCP, the finite temperature properties of the system are modified and may reveal, for instance, deviations from the Fermi-liquid behavior or unconventional superconductivity.¹

Intermetallics associating intermediate valent Yb with a magnetic 3d element (mainly Fe or Mn) are still scarcely studied.⁹⁻
¹⁴ The interplay between unstable 4f shell and magnetic 3d electrons may lead to new and intriguing phenomena. In particular, it has been shown that in $\text{YbMn}_6\text{Ge}_{6-x}\text{Sn}_x$, though the Yb physics still obeys a Doniach-like picture,¹³ the strong Mn-Yb interaction yields high temperature magnetic ordering of Yb (up to ~ 125 K),¹³ unusual thermal dependence of the Yb valence^{11,12} and high-temperature quantum critical effects deep inside the intermediate valent regime ($v \sim 2.77$)¹⁴.

In the search for other intermetallic systems involving Yb and a magnetic 3d element with potentially rich phenomena to explore, the published data on the non-stoichiometric $\text{YbMn}_{-0.17}\text{Si}_{-1.89}$ compound caught our attention.¹⁵ This phase, whose crystal structure is still a matter of debate,^{15,16} magnetically orders at ~ 4.5 K. The authors suggested that Yb carrying a local moment could explain the low-field negative magnetization observed below this temperature.¹⁵ At higher temperature, the Curie-Weiss law shows a change of slope near ~ 200 K, which has been tentatively interpreted as being due to an Yb valence change. Finally, specific heat measurements point to a heavy-fermion material and non-Fermi-liquid behavior.

In the present paper, we reinvestigate the crystal structure of this non-stoichiometric phase from single-crystal x-ray diffraction and investigate the temperature and pressure dependence of the Yb valence from x-ray absorption spectroscopy measurements at the Yb L_3 edge. External pressure is a clean parameter to vary the 4f - conduction electron hybridization and to access new ground states.^{1,17,18}

II. EXPERIMENTAL DETAILS

Single crystals of $\text{YbMn}_{-0.17}\text{Si}_{-1.89}$ were grown by the flux method using In as a flux. The first stage consisted in loading the constituting elements (9 mmol of Yb, 6 mmol of Mn, 18 mmol of Si, and 135 mmol of In) in a fused silica tube, which was sealed under a pressure of 0.2 bar of pure argon. The silica ampoule was subsequently placed into a resistive vertical furnace

for melting. The reactants were heated up to 1273 K at a rate of 97.5 K/h and kept at this temperature for 5 h in order to promote proper homogenization. Then the temperature was reduced down to 1123 K at a rate of 75 K/h, and maintained there for 48 h. Finally, the system was slowly cooled down to 323 K during 48 h. The In flux was isolated from the reaction product by heating up to 623 K, followed by a subsequent centrifugation. Using this method, several single crystals of $\sim 0.1 \text{ mm}^3$ were obtained.

Single crystal x-ray diffraction data were collected on a Bruker DUO-APEX2 CDD area detector diffractometer at 300 K using a Mo K_α radiation ($\lambda = 0.71073 \text{ \AA}$). Data reduction was accomplished using SAINT V8.34a.¹⁹ The substantial redundancy in data allowed a semiempirical absorption correction (SADABS 2012-1)²⁰ to be applied, based on multiple measurements of equivalent reflections. The structure was solved by the intrinsic phasing method from SHELXT program,²¹ developed by successive difference Fourier syntheses, and refined by full matrix least squares on all F^2 data using SHELX via Olex2 interface.²²

X-ray Absorption measurements at the Yb L_3 edge were performed at the ODE beamline of the SOLEIL synchrotron (Saint-Aubin).²³ Absorption spectra were recorded with dispersive mode at ambient pressure between 300 and 10 K in a He circulating cryostat using a position sensitive CCD detector. Absorption spectra were also collected at 10 K under external pressure up to $\sim 37 \text{ GPa}$ in a diamond anvil cell with silicon oil as pressure transmitting medium. The pressure was determined using the shift of the ruby R1 fluorescence line.²⁴ The spectra have been normalized to a step-edge of unity.

III. RESULTS AND DISCUSSION

A. X-ray diffraction

The crystal structure of the titled compound was previously refined and described by two groups. The original refinement by Norlidah *et al.*¹⁶ revealed an orthorhombic lattice (SG $Cmcm$) while in 2013 Peter *et al.*¹⁵ refined the structure in the monoclinic lattice with a non-centrosymmetric space group ($P2_1$). The purpose of the latter authors to use a lower symmetry was to avoid some short interatomic distances and large anisotropic displacements (especially for Si3 atoms, located on a 16(h) position and deviated from a 4(c) site) resulting from the Norlidah *et al.* analysis. Here, we refined the same set of data in both lattices. The refined crystal parameters of the compound are given in Table I. Both refinements yielded identical chemical composition $\text{YbMn}_{-0.17}\text{Si}_{-1.89}$ (see Tables II and III). Information about anisotropic displacement parameters and main interatomic distances can be found in the supplementary material for both lattices (Tables S1 to S4). The structure can be described as stacking of three blocks of AlB_2 separated by one BaAl_4 block along the b axis as presented in figure 1 in the orthorhombic lattice (see figures S1 and S2 for representation in the monoclinic one).

TABLE I. Crystal data and structure refinement for YbMn-0.17Si-1.89

	Orthorhombic lattice	Monoclinic lattice
Empirical formula	Mn _{0.17} Si _{1.89} Yb	Mn _{0.18} Si _{1.88} Yb
Formula weight	235.67	235.53
Temperature/K	299.25	299.25
Crystal system	orthorhombic	monoclinic
Space group	<i>Cmcm</i>	<i>P2₁</i>
a/Å	4.0179(2)	4.0179(2)
b/Å	28.6661(12)	3.8434(2)
c/Å	3.8435(2)	14.4734(7)
α /°	90	90
β /°	90	97.9865(16)
γ /°	90	90
Volume/Å ³	442.68(4)	221.336(19)
Z	8	4
$\rho_{\text{calc}}/\text{cm}^3$	7.072	7.068
μ/mm^{-1}	43.758	43.767
F(000)	806.0	403.0
Crystal size/mm ³	0.244 × 0.081 × 0.043	0.091 × 0.091 × 0.045
Radiation	MoK α (λ = 0.71073)	MoK α (λ = 0.71073)
2 Θ range for data collection/°	5.684 to 93.976	5.684 to 93.866
Index ranges	-8 ≤ h ≤ 8, -58 ≤ k ≤ 58, -7 ≤ l ≤ 7	-8 ≤ h ≤ 8, -7 ≤ k ≤ 7, -29 ≤ l ≤ 29
Reflections collected	12959	13032
Independent reflections	1196 [R_{int} = 0.0280, R_{sigma} = 0.0145]	3994 [R_{int} = 0.0243, R_{sigma} = 0.0247]
Data/restraints/parameters	1196/0/39	3994/1/66
Goodness-of-fit on F ²	1.261	1.144
Final R indexes [$I \geq 2\sigma(I)$]	R_1 = 0.0168, wR_2 = 0.0341	R_1 = 0.0243, wR_2 = 0.0574
Final R indexes [all data]	R_1 = 0.0179, wR_2 = 0.0344	R_1 = 0.0274, wR_2 = 0.0588
Largest diff. peak/hole / e Å ⁻³	1.81/-2.52	1.82/-5.59
Flack parameter		0.50(2)

However, refinements in the orthorhombic lattice are slightly more satisfactory: 1) the R_1 value is lower in this symmetry = 1.68 % (vs. 2.43 % in the monoclinic setting); 2) The refinement in the $P2_1$ space group reveals a Flack parameter of 0.5, suggesting the use of a centrosymmetric space group is required; 3) The anisotropic displacement for silicon atoms are similar in both structures. The largest atomic displacement parameter in orthorhombic is $U_{33} = 0.056(3)$ for Si4 (Table S1), while it is $U_{22} = 0.065(4)$ for Si4 in monoclinic (Table S2).

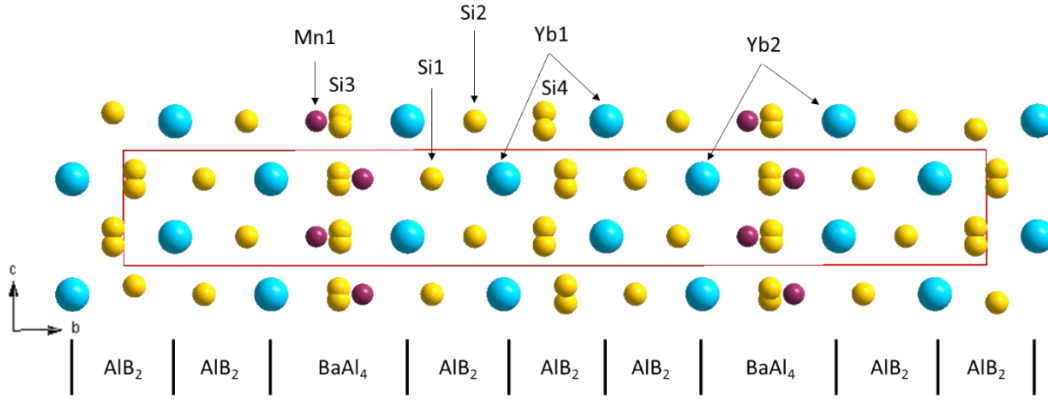


FIG. 1. Representation of the $\text{YbMn}_{-0.17}\text{Si}_{-1.89}$ structure in the orthorhombic lattice.

In addition, the too short Mn-Si distances in the orthorhombic system no longer exist if one assume a local order of the partially occupied Si3 and Mn1 positions, as firstly proposed by Norlidah *et al.*¹⁶ (figure 2a). In such a case, the short Mn-Si distances (1.8936(20) and 2.0298(38) Å) have not to be considered and only remain physically sound Mn-Si distances (2.2396(20) and 2.3089(38) Å). With this model, the Si3-Si3 bond distances are in the range 2.3066(46)-2.7824(50) Å. Table S3 gives the main interatomic distances in the orthorhombic structure. The unrealistic and non-existing ones are marked in italic.

TABLE II. Atomic coordinates for $\text{YbMn}_{-0.17}\text{Si}_{-1.89}$ in $Cmcm$

Atom	Position	x	y	z	occupancy
Yb1	4c	0	0.5595(0)	1/4	1
Yb2	4c	0	0.3291(0)	1/4	1
Mn1	4c	0	0.2232(0)	1/4	0.351(3)
Si1	4c	0	0.1427(0)	1/4	1
Si2	4c	0	0.9069(0)	1/4	1
Si3	16h	0.5375(10)	0.2509(1)	0.2016(5)	0.25
Si4	8f	0.1989(1)	0.0124(1)	0.8244(9)	0.387(5)

TABLE III. Atomic coordinates for $\text{YbMn}_{-0.17}\text{Si}_{-1.89}$ in $P2_1$

Atom	Position	x	y	z	occupancy
Yb1	2a	0.94046(4)	0.4506(3)	0.88092(2)	1
Yb2	2a	0.82915(4)	0.95252(6)	0.65831(2)	1
Mn1	2a	0.2768(5)	0.459(2)	0.55358(12)	0.356(4)
Si1	2a	0.3572(3)	0.4519(13)	0.71460(9)	1
Si2	2a	0.5932(3)	0.4514(12)	0.18631(10)	1
Si3	2a	0.2505(7)	0.947(3)	0.50193(13)	1
Si4	2a	0.5125(6)	0.5272(11)	0.02473(18)	0.757(12)

There are two independent Yb sites and their coordination environment is shown in figures 2b-2d. The local environment of Yb1 is made of 20 neighbors, 8 of which are Si ones and 12 Yb neighbors (CN = 20). The Yb2 is surrounded by 10 Si, 6 Yb and has 5 Mn1 sites but with an occupancy ratio of 0.35, that is an average of 1.75 Mn first neighbors. Figures 2c and 2d represent two possible Yb2 environments in the Norlidah *et al.* model¹⁶, with respectively 2 and 1 Mn atoms (CN = 18 and 17).

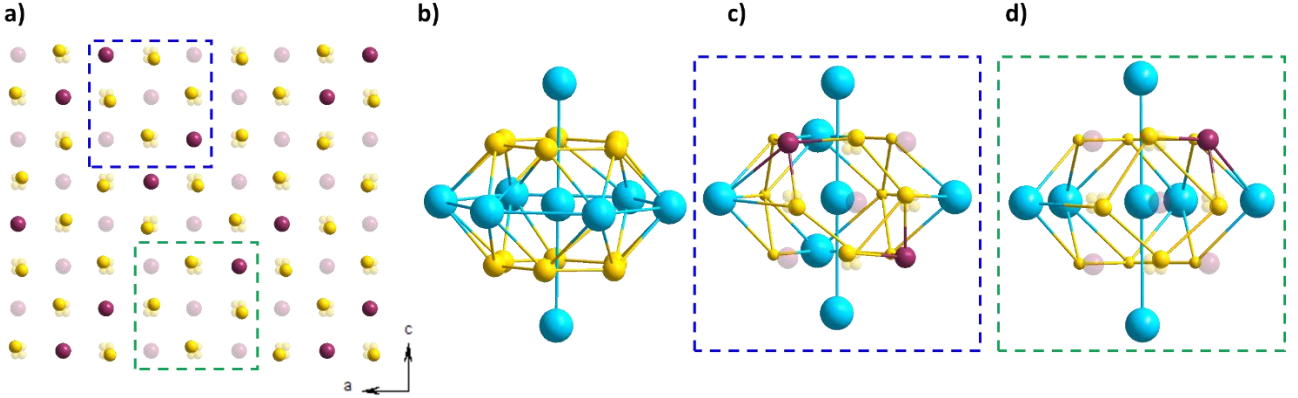


FIG. 2. a) Representation of the hypothetical ordering of Mn1 and Si3 atoms in the BaAl₄ layers in *Cmc21*; b) Environment of the Yb1 atom; c) and d) Two possible environments of the Yb2 atom due to local order of Mn atoms represented in a).

B. X-ray absorption

The ambient pressure Yb L₃ XANES spectra recorded at several temperatures between 300 and 10 K are shown in figure 3. They have typical shape for intermediate valent Yb and show only little changes with temperature. Each spectrum consists of a main structure near 8.948 keV and a shoulder near 8.941 keV that correspond, respectively, to transitions from the initial Yb intermediate valent state to the final states of mainly $2p^54f^{13}$ (trivalent) and $2p^54f^{14}$ (divalent) character. The spectra were fitted using two pseudo-Voigt functions for the two structures and two arctangent-type step functions due to the $2p_{3/2} \rightarrow$ continuum transitions (figure S3). The weight of each valence configuration ($4f^{13}$ and $4f^{14}$) in the initial valence state is proportional to the peaks surface area S_3 (trivalent) and S_2 (divalent). The Yb valence was derived from $(2S_2+3S_3)/(S_2+S_3)$.^{25,26} The estimated accuracy on the Yb valence is ± 0.02 . The inset of figure 3 shows the temperature dependence of the extracted average Yb valence which is found constant within the error bars close to $v_{av} \sim 2.42$. The measured Yb valence is the average of the valence of the two Yb crystallographic sites of identical multiplicity. As described in section III.A, the two crystallographic Yb sites have similar coordination numbers and interatomic distances, which suggest they have close Yb valences.

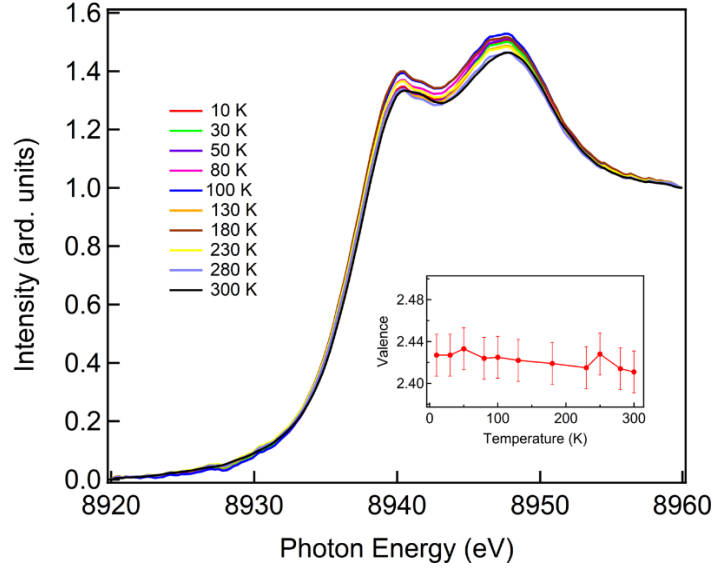


FIG. 3. Yb L_3 XANES spectra of $\text{YbMn}_{-0.17}\text{Si}_{-1.89}$ between 300 and 10 K. The inset shows the temperature dependence of the extracted average Yb valence v_{av} .

It was recently shown that the scaling between the Kondo temperature T_K and $(3-v)$ obeys a power law $(3-v) \approx AT_K^\alpha$, with $\alpha = 2/3$ and $A = 1/200$.²⁷ From the average measured valence $v_{\text{av}} \sim 2.42$, we estimate the average Kondo temperature to be ~ 1250 K. Such a high Kondo temperature is consistent with the lack of thermal dependence of the measured Yb valence below 300 K since, in the single impurity Anderson model, the Yb valence rapidly decreases at $T < T_K$ before taking a constant value at low enough temperature.^{28,29} For instance, the Yb valence was found constant $v \sim 2.3$ - 2.4 below 300 K in $\text{YbGa}_x\text{Si}_{2-x}$ ($1.12 \leq x \leq 1.49$)³⁰ or in YbCu_5 .³¹ Conversely, in the extreme hypothesis of two Yb sites in $\text{YbMn}_{-0.17}\text{Si}_{-1.89}$ having very different Yb valences, say ~ 2.0 and ~ 2.84 , the Kondo temperature of the most trivalent site would be ~ 180 K and we should have observed a decrease of the average Yb valence upon cooling below 300 K. Hence, taken together, these remarks suggest that the two Yb crystallographic sites in $\text{YbMn}_{-0.17}\text{Si}_{-1.88}$ have similar Yb valences around $v \sim 2.4 \pm 0.1$.

Yb atoms in such strongly intermediate valent state (*i.e.* with a high T_K) cannot bear local moment at room temperature and below, since local moment behavior on Yb is expected only for temperatures higher than T_K .^{1,32} Consequently, it is hardly conceivable that Yb participates in the low temperature antiferromagnetic ordering ($T_N = 4.5$ K) reported in Ref. 15 and only Mn magnetic moments can be involved. Further, the occurrence of a Curie-Weiss behavior in the 50-300K temperature range originating from local moment on Yb, as reported in Ref. 15, is highly questionable. We note that in their analysis Peter *et al.* seem not to have considered an effective moment on Mn.¹⁵ Whatever, our temperature dependent XANES data do not evidence a valence change occurring near ~ 200 K, which was proposed in Ref. 15.

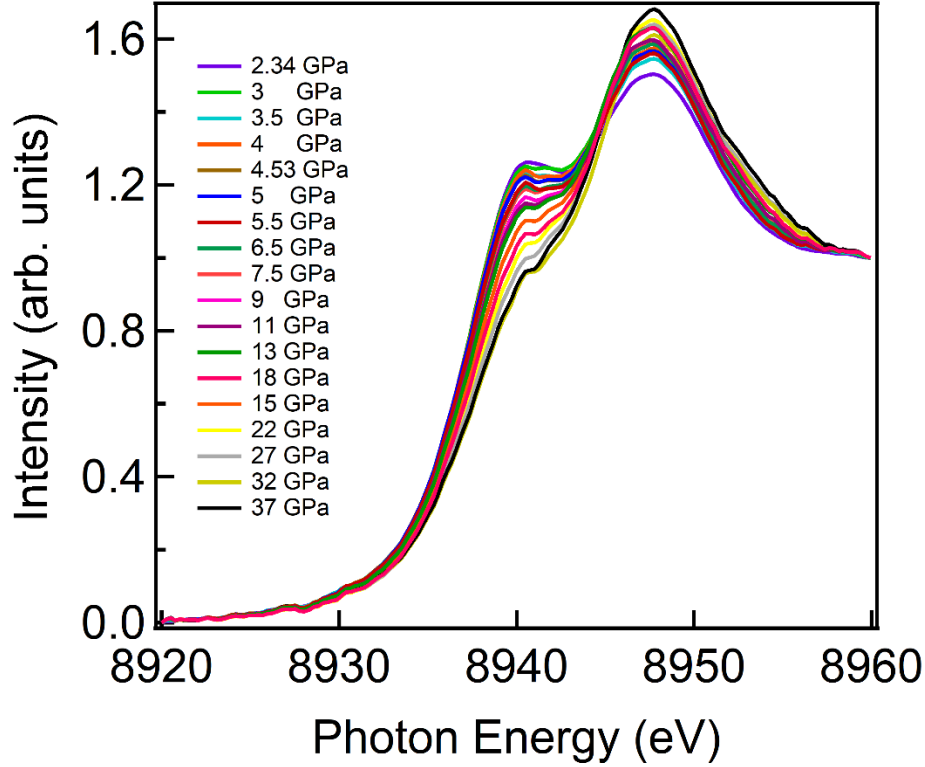


FIG. 4. Pressure dependence of the XANES spectra of $\text{YbMn}_{-0.17}\text{Si}_{-1.89}$ at 10 K.

The Yb L_3 XANES spectra recorded at 10 K upon increasing external pressure up to ~ 37 GPa are shown in figure 4. As expected, they show a clear spectral weight transfer from the divalent to the trivalent component upon pressure increase, as observed in many others Yb-based intermetallics,^{10,17,18} since the pressure increase promotes the trivalent ($4f^{13}$) state of lower atomic volume than the divalent one ($4f^{14}$). The pressure dependent average Yb valence v_{av} extracted from the fits is plotted in figure 5. The valence change is rather sluggish. Even at the highest pressure of the measurements ($P \sim 37$ GPa), Yb atoms are still in a strongly intermediate valent regime far from trivalency ($v_{\text{av}} \sim 2.63$) and the Yb valence does not saturate. The average Yb valence increases at a rate of $\partial v_{\text{av}}/\partial P \sim 0.01 \text{ GPa}^{-1}$ up to $P \sim 8$ GPa while $\partial v_{\text{av}}/\partial P$ reduces to $\sim 0.003 \text{ GPa}^{-1}$ at higher pressures. These rates are almost one order of magnitude lower than those observed in YbNiGe_3 of close ambient pressure valence.¹⁷ The behavior of $\text{YbMn}_{-0.17}\text{Si}_{-1.89}$ resembles that of YbNiGa_4 where $v \sim 2.44$ at $P = 0$ GPa and $v \sim 2.67$ at $P \sim 40$ GPa.¹⁸ No strong anomaly possibly associated with a first-order valence transition is observed, hinting that the pressure-induced valence change is not linked to a dramatic volume change such reported for YbMn_2Ge_2 .¹⁰ Change of slope in the pressure dependence of the Yb valence may be indicative of a QCP.¹⁷ Here, however, the Yb valence at the slope change is too low ($v_{\text{av}} \sim 2.52$ at $P \sim 8$ GPa) to be due to the magnetic instability of Yb since, to the best of our knowledge, local magnetism on Yb occurs at best for $v > 2.7$.^{4,6,13,14} Even under the highest applied pressure of ~ 37 GPa, the Yb atoms in $\text{YbMn}_{-0.17}\text{Si}_{-1.89}$ are still too much

hybridized ($v_{av} \sim 2.63$) to magnetically order. Hence, the Yb atoms are still distant from their magnetic instability and the corresponding quantum criticality. Due to the absence of high pressure X-ray data or high pressure temperature dependent XANES data, it cannot however be excluded that the valence of Yb1 and Yb2 may evolve differently at high pressure with possibly one of the two being then closer to its magnetic instability.

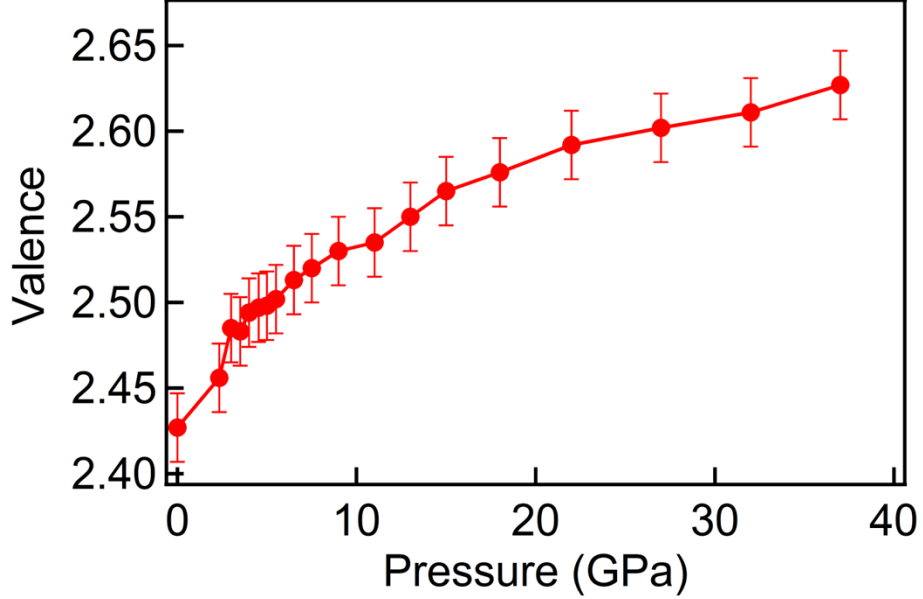


FIG. 5. Pressure dependent average Yb valence in $\text{YbMn}_{-0.17}\text{Si}_{-1.89}$ at 10 K.

IV. CONCLUSION

To summarize, the crystal structure of $\text{YbMn}_{-0.17}\text{Si}_{-1.89}$ can be described in an orthorhombic ($Cmcm$) or a non-centrosymmetric monoclinic ($P2_1$) cell, though the orthorhombic one together with a local order of the Mn1 and Si3 atoms yields slightly more satisfactory results. In both cases, Yb atoms locate on two sites of identical multiplicity, with close coordination numbers and interatomic distances. Below 300 K, the average Yb valence is found independent of temperature ($v_{av} \sim 2.42$). The close atomic environment of the two Yb sites and the lack of thermal dependence in the average Yb valence suggest their individual valence is similar, close to $v \sim 2.4$. Such strongly hybridized Yb can hardly bears a local moment. Thus, the previously identified magnetic properties of $\text{YbMn}_{-0.17}\text{Si}_{-1.89}$ likely arise solely from the Mn sublattice. The average Yb valence smoothly varies with pressure and remains well below trivalency even at the highest applied pressure of 37 GPa ($v_{av} \sim 2.63$), suggesting that Yb atoms are still far from their magnetic instability and the associated quantum critical effects.

SUPPLEMENTARY MATERIALS

See the supplementary material for the atomic displacement parameters and main interatomic distances tables in orthorhombic and monoclinic settings and for representations of the crystal structure and local Yb environment in the monoclinic lattice.

ACKNOWLEDGMENTS

We acknowledge the French Synchrotron facility SOLEIL (Saint-Aubin, France) for the allocated beam time (exp. n° 20201389).

AUTHOR DECLARATIONS

Conflict of Interest

The authors have no conflicts to disclose.

Author Contributions

Bodry Tegomo Chiogo: Formal Analysis (equal); Visualization (equal); Funding Acquisition (supporting); Writing – review and editing (equal). **Nicolas P. Martin:** Formal Analysis (equal); Visualization (equal); Writing-Original Draft Preparation (supporting); Writing – review and editing (equal). **Léopold V.B. Diop:** Resources (lead); Writing-Original Draft Preparation (supporting); Writing – review and editing (equal); **Bernard Malaman:** Formal Analysis (supporting). **Daniel Malterre:** Funding Acquisition (lead); Formal Analysis (supporting); Writing – review and editing (equal). **François Baudalet:** Data curation (lead); Resources (supporting). **Lucie Nataf:** Data curation (lead); Resources (supporting). **Thomas Mazet:** Formal Analysis (supporting); Conceptualization (lead); Writing-Original Draft Preparation (lead); Writing – review and editing (equal).

DATA AVAILABILITY

The data that support the findings of this study are available from the corresponding author upon reasonable request.

REFERENCES

¹P. Coleman, Heavy Fermions: electrons at the edge of magnetism in Handbook of Magnetism and Magnetic Materials (Wiley, New York, 2007).

- ²S. Doniach, *Physica B* **91**, 231 (1977).
- ³N. Tsujii, L. Keller, A. Dönni and H. Kitazawa, *J. Phys.: Condens. Matter* **28**, 336002 (2016).
- ⁴S. Suzuki, K. Takubo, K. Kuga, W. Higemoto, T.U. Ito, T. Tomita, Y. Shimura, Y. Matsumoto, C. Bareille, H. Wadati, S. Shin, and S. Nakatsuji, *Phys. Rev. Res.* **3**, 023140 (2021).
- ⁵J. Custers, P. Gegenwart, C. Geibel, F. Steglich, P. Coleman, and S. Paschen, *Phys. Rev. Lett.* **104**, 186402 (2010).
- ⁶T. Tomita, K. Kuga, Y. Uwatoko, P. Coleman, S. Nakatsuji, *Science* **349**, 506 (2015).
- ⁷Q. Si and S. Paschen, *Phys. Status Solidi B* **250**, 425 (2013).
- ⁸S. Watanabe and K. Miyake, *J. Phys.: Condens. Matter* **23**, 094217 (2011).
- ⁹H. Yamaoka, I. Jarrige, N. Tsujii, J.-F. Lin, T. Ikeno, Y. Isikawa, K. Nishimura, R. Higashinaka, H. Sato, N. Hiraoka, H. Ishii, and K.-D. Tsuei, *Phys. Rev. Lett.* **107**, 177203 (2011).
- ¹⁰R.S. Kumar, A. Svane, G. Vaitheeswaran, Y. Zhang, V. Kanchana, M. Hofmann, S.J. Campbell, Y. Xiao, P. Chow, C. Chen, Y. Zhao, and A. Cornelius, *Inorg. Chem.* **52**, 832 (2013).
- ¹¹T. Mazet, D. Malterre, M. François, C. Dallera, M. Grioni, and G. Monaco, *Phys. Rev. Lett.* **111**, 096402 (2013).
- ¹²T. Mazet, D. Malterre, M. François, L. Eichenberger, M. Grioni, C. Dallera, and G. Monaco, *Phys. Rev. B* **92**, 075105 (2015).
- ¹³L. Eichenberger, D. Malterre, B. Malaman, and T. Mazet, *Phys. Rev. B* **96**, 155129 (2017).
- ¹⁴L. Eichenberger, A. Magnette, D. Malterre, R. Sibille, F. Baudelet, L. Nataf, and T. Mazet, *Phys. Rev. B* **101**, 020408(R) (2020)
- ¹⁵S.C. Peter, C.D. Malliakas, and M.G. Kanatzidis, *Inorg. Chem.* **52**, 4909 (2013).
- ¹⁶N.M. Norlidah, I. Ijjaali, G. Venturini, B. Malaman, *J. Alloys Compd.* **278**, 246 (1998).
- ¹⁷H. Sato, H. Yamaoka, Y. Utsumi, H. Nagata, M.A. Avila, R.A. Ribeiro, K. Umeo, T. Takabatake, Y. Zekko, J. Mizuki, J.-F. Lin, N. Hiraoka, H. Ishii, K.-D. Tsuei, H. Namatame, and M. Taniguchi, *Phys. Rev. B* **89**, 045112 (2014).
- ¹⁸Z.E. Brubaker, R.L. Stillwell, P. Chow, Y. Xiao, C. Kenney-Benson, R. Ferry, D. Popov, S.B. Donald, P. Söderlind, D.J. Campbell, J. Paglione, K. Huang, R.E. Baumbach, R.J. Sieve, and J.R. Jeffries, *Phys. Rev. B* **98**, 214115 (2018).
- ¹⁹SAINT Plus Version 8.34a, Bruker Analytical X-rays Systems, Madison, WI, (2013).
- ²⁰G. Sheldrick, SADABS, Bruker-Siemens area detector absorption and other correction, Version 2008/1, (2008).
- ²¹G. Sheldrick, *Acta Cryst. A* **71**, 3 (2015).
- ²²O. V. Dolomanov, L. J. Bourhis, R. J. Gildea, J. A K. Howard and H. Puschmann, *J. Appl. Crystallogr.* **42**, 339 (2009).
- ²³F. Baudelet, L. Nataf, and R. Torchio, *High Press. Res.* **31**, 136 (2011).
- ²⁴K. Syassen, *High Press. Res.* **28**, 75 (2008).
- ²⁵J. Röhler, *J. Magn. Magn. Mater.* **47&48**, 175 (1985).
- ²⁶L. Eichenberger, G. Venturini, B. Malaman, L. Nataf, F. Baudelet and T. Mazet, *J. Alloys Compd.* **695**, 286 (2017).

- ²⁷K. Kummer, C. Geibel, C. Krellner, G. Zwicknagl, C. Laubschat, N.B. Brookes and D.V. Vyalikh, *Nat. Commun.* **9**, 2011 (2018).
- ²⁸N.E. Bickers, D.L. Cox, and J.W. Wilkins, *Phys. Rev. B* **36**, 2036 (1987).
- ²⁹L.H. Tjeng, S.-J. Oh, E.-J. Cho, H.-J. Lin, C.T. Chen, G.-H. Gweon, J.-H. Park, J.W. Allen, T. Suzuki, M.S. Makivic, and D.L. Cox, *Phys. Rev. Lett.* **71**, 1419 (1993).
- ³⁰N. Tsujii, M. Imai, H. Yamaoka, I. Jarrige, H. Oohashi, T. Tochio, K. Handa, J. Ide, H. Atsuta, Y. Ito, H. Yoshikawa, and H. Kitazawa, *Chem. Mater.* **22**, 4690 (2010).
- ³¹E. Bauer, R. Hauser, L. Keller, P. Fisher, O. Trovarelli, J.G. Sereni, J.J. Rieger, and G.R. Stewart, *Phys. Rev. B* **56**, 711 (1997).
- ³²Y. Kishimoto, Y. Kawasaki, T. Ohno, *Phys. Lett. A* **317**, 308 (2003).